1. Abstract

As biomedical visual data in 3D spatial spaces collected at an increasing speed, there is a growing demand for accurate and efficient application for comparative data analysis. For comparing purpose, mesh subdivision techniques are commonly used to adaptively generate and amplify tiny differences. Compared with current methods, the smoothing methods for each subdivision algorithm will moderate features in the original mesh. In this paper, we propose an edge features focused mesh subdivision method, which generates a visually sensitive and precise result compared with commonly used subdivision methods.

2. Introduction

Nowadays, three dimensional CT (3D CT) reconstruction [12][13][14][15][26][27][28], as advanced clinical auxiliary computer graphical technique, has obvious advantages over ordinary radiography and conventional tomography. The technique is used for presenting facial bones and their connections, confirmation of borderline or size of the diseased tissues and their relation to the adjacent tissues. With the aid of 3D bio-images and bio-models, diagnosis and operations on tissues or bones will be more accurate. Moreover, substantial effort has been make around world to determine spatial expression patterns of genes in mammalian genome [18][19][22][23][24][25] using experimental techniques such as in situ hybridization (ISH)[17]. Performing ISH on multiple subjects yields expression images of various genes over the common anatomical structure. Comparing these images reveals the spatial relations between genes, which are often key to understanding their functional relations [16][20][21].

The advance of using ubiquitously Computer Graphics including 3D spatial and triangular meshes [29][30][31] to expose nicety of bioinformation has created an ever-titanic amount of spatial data (in the form of 2D medical images, and 3D bio-models) which requires efficient and accurate process and analysis. The anatomical differentiations among these biomedical models aggravate the computational challenges involved in visual and medical comparison among data collected from different modes [6].

A typical method to differentiate tiny divergence is using precision amplification techniques, mesh subdivision is one of the implementation. Using subdivision meshes, spatial data can be organized into multi-resolution versions, on which visual comparison and diagnosis will have a higher performance. Meanwhile, the multi-resolution structure of a subdivision mesh further gives rise to fast algorithms for processing [6].

Commonly used mesh subdivision methods including Butterfly method [3], Loop subdivision [1], and Catmull-Clark subdivision [2], whose experimental result will be illustrate in Figure 1. Moreover, Xie [32] provide a solid-shell element based triangular subdivision to avoid interpenetration. Liu [33] introduced a dense reconstruction algorithm for mesh subdivision. Amresh [7] developed a subdivision scheme derivate from Loop scheme and

using watershed segmentation. Dirc Rose [8] proposed an adaptive process that stores the next splitting vertex and temporary triangle based on Modified Butterfly scheme. Kobbelt [9] developed refinement for both his Kobbelt scheme and newly introduced $\sqrt{3}$ subdivision. Seeger [10] introduced a subdivision scheme based on Butterfly Scheme using quark, while Xu and Kondo's scheme [11] is based on Doo-Sabin scheme. In their method, subdivision is controlled by the faces of the original mesh.

In this paper, we propose three mesh subdivision methods including Edge Sensitive Mesh subdivision, Model-related Noise Wave Eliminated Edge Sensitive Mesh Subdivision, and Keypoints-based Edge Sensitive Mesh Subdivision to keep edge features of original meshes while give out a more adaptive derivative. Subdivision Result will be compared by using the same mesh after same time of iterations, whose visual difference is unambiguously discerned.

The rest of the paper is organized as follows: In Section 3, we present the basic idea of Edge Sensitive Mesh Subdivision, and its improved version to efface model-related noise wave on the mesh. In Section 4, we introduce our previous work on 3D imbalanced keypoints detection [5] and using detected keypoints as a guideline to optimize subdivision result. Experimental comparison and conclusion will be demonstrated in Section 5 and Section 6, respectively.

3. Edge Sensitive Mesh Subdivision

In this section, we provide two methods for triangular mesh subdivision: Edge Sensitive Mesh Subdivision, and Model-related Noise Wave Eliminated Edge Sensitive Mesh Subdivision. Both methods follow the iterated scheme of subdivision plus smoothing.

3.1. Feature Sensitive Mesh Subdivision

Loop's method can be expressed in terms of linear subdivision and an averaging scheme to approximate a spherical surface, which will efface edges and vertices features. The phenomenon is common when applying Catmull method[2], and Butterfly method[3]. When the mesh is rigid, these iterations will fail as illustrated in Figure 1. To moderate the feature wastage after subdivision and highlight original edge and vertex features, we provide a feature sensitive mesh subdivision.

a b c d e

Figure 1 a) original mesh. b) Loop Subdivision. c) Catmull Subdivision. d) Butterfly Subdivision. e) Feature Sensitive Mesh Subdivision. Except a), all these subdivisions have been applied five times on

the original mesh.

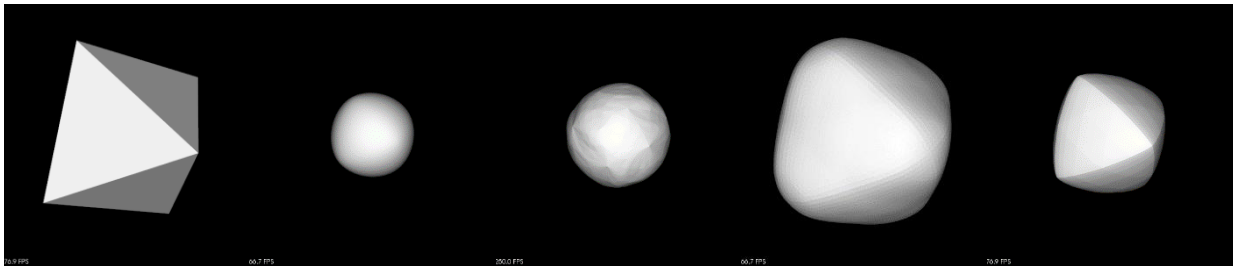

a b c d e

Figure 2 a) original mesh. b) Loop Subdivision. c) Catmull Subdivision. d) Butterfly Subdivision. e) Feature Sensitive Mesh Subdivision. Except a), all these subdivisions have been applied five times on the original mesh.

Our proposed method implements linear one to four triangular mesh subdivisions to increase the details in a mesh as illustrated in Figure 3, and smooths by proposed smoothing algorithm to accomplish surface fitting after subdivision while actualize shape retention.

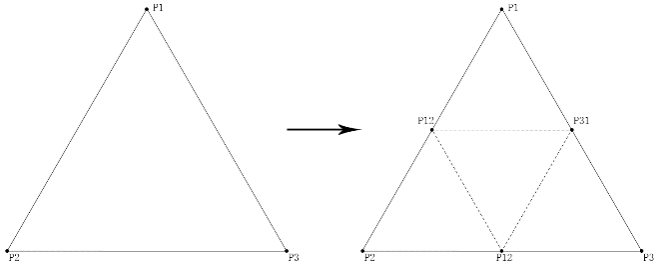

Figure 3 Linear 1 to 4 subdivision of triangles for triangular subdivision schemes.

Denote the original mesh as M_i. To perform linear triangular subdivision, we insert middle vertices on the edge of each triangle to the hash map $H_n(v_i,h_i)$ for storing vertices coordination v_i and their handles h_i as corresponding hash key. For each vertex on mesh $\{v_1,v_2,\dots,v_n\}$, check if the generated middle edge point v_k is already in the map. If so, get its handle h_k for the on-coming face generation, else, insert the point v_k into the mesh and create its handle h_k while update vertices hash map $H_{n+1}(v_i,h_i)$. Finally, form the new triangular surfaces using vertex handles geometrically anticlockwise, and eliminate elder redundant faces simultaneously. Each triangle will then be split into four sub-triangles and original mesh M_i is subdivided to M_{i+1}.

Smoothing for triangular meshes will be applied on not only the previous vertices on M_i but all vertices on the generated mesh M_{i+1} whose two-ring vertex set is derived from one-ring vertices of previous mesh M_i as illustrated in Figure 4. For each vertex on M_{i+1}, we use a one-ring neighbor weighted centroid method for averaging shown in Figure 5. The weight of each neighbor β is decided by the number of one-ring neighbors n.

$$\beta = \frac{5}{8} - \left(\frac{3}{8} + \frac{1}{4}\cos\frac{2\pi}{n}\right)^2$$

Equation 1

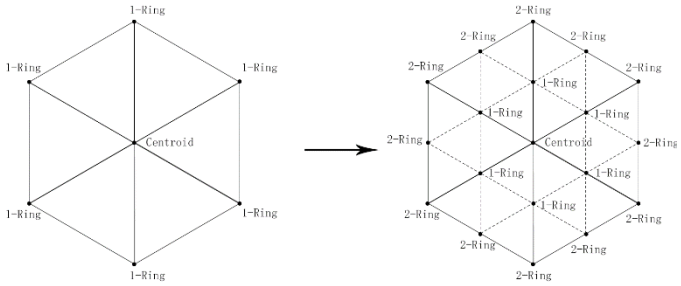

Figure 4 One-ring vertices Derivative

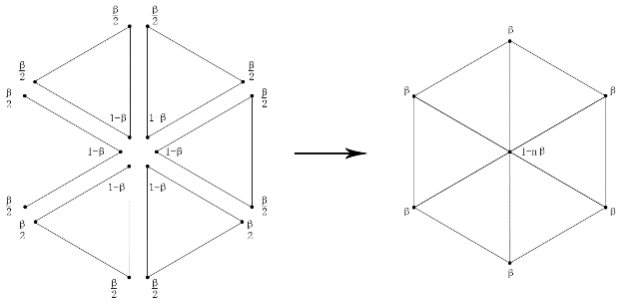

Figure 5 One-ring neighbor weighted centroid method for triangular vertices

3.2. Advanced Feature Sensitive Mesh Subdivision

By using Feature Sensitive Mesh Subdivision, an edge and vertex sensitive result is generated. But the method will generate model-depend wavelike noise on the mesh, as illustrated in Figure 6.

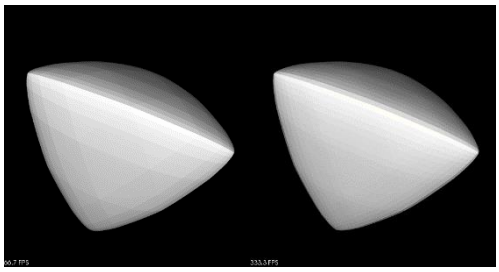

a b

Figure 6 a) Model-depend wavelike noise. b) Advanced Feature Sensitive Mesh Subdivision. Both subdivisions have been applied five times on the original mesh.

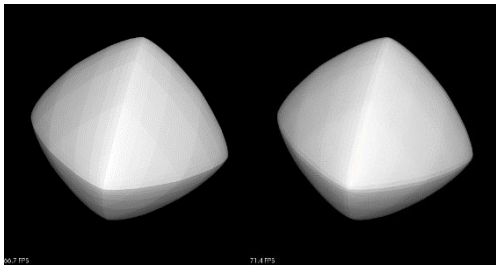

a b

Figure 7 a) Model dependent noise waves on the mesh. b) Advanced Edge Sensitive Mesh Subdivision. Both subdivisions have been applied five times on the original mesh.

We propose an Advanced Feature Sensitive Mesh Subdivision which is a combination of Feature Sensitive Mesh Subdivision and Smoothness-focused Mesh Subdivision. The Subdivision scheme consists of several iterations of Feature Sensitive Subdivision and an iteration of Smoothness-focused Mesh Subdivision at the end of algorithm. The implementation of Smoothness-focused Mesh Subdivision resembles the Feature Sensitive Mesh Subdivision, except the generation of edge points and smoothing operator.

Unlike the middle edge points generation in Feature Sensitive Subdivision, the edge points in the last iteration of Advanced Edge Sensitive Subdivision are generated based on weighted neighbors illustrated in Figure 8, where directly connected vertices take up a greater weight, say 3/8 each, and indirect weight slightly less, say 1/8 each.

Neighbor vertices for smoothing method depends on previous one-ring vertices on M_i, which is different from vertex pickup in the implementation of Feature Sensitive Subdivision, but not newly generated vertices on M_{i+1}. The weight of each neighbors follows the same principle introduced in Feature Sensitive Mesh Subdivision.

4. Keypoints-based Edge Sensitive Mesh Subdivision

The result of subdivision should depend on the feature of meshes, which will lead a better subdivision result and higher efficiency. In this section, we propose a detection of imbalanced vertices in 3D meshes, and using detected keypoints to guide subdivision procedure.

4.1. Imbalanced Vertices Detection

We first propose a vertex geometric feature based operator, which is a two-dimensional implementation of keypoints selection. We extend Li's [4] previous work on imbalanced keypoints detection to triangular meshes.

The basic idea is using projections to transform 3D geometric features to two-dimensional spaces. Let $\mathrm{M}(\mathrm{V},\mathrm{F},\mathrm{N}_F)$ be a triangular mesh where V is the set of vertices, F is the set of faces, and N_F represents the set of face normals. Suppose a projection P_T will project any vector to the plane T, 3D geometric mesh features will be project to two-dimension when T is the tangent plane of mesh vertices in V.

Imbalanced point detection in 2D images aims to minimize the occurrences of edge points [4]. Denote I a gray value image, p a local point, $\theta_i = \frac{(i-1)2\pi}{N}$, and $\mathrm{l}_i = (\cos\theta_i, \sin\theta_i)$ for $\mathrm{i} = 1, 2, \ldots, \mathrm{N}$. Denote $\frac{\partial \mathrm{I}}{\partial \mathrm{l}_i}(p)$ a directional derivative of p along l_i direction. We cluster $\left\{\frac{\partial \mathrm{I}}{\partial \mathrm{l}_i}(p)\right\}_{i=1}^{N}$ into two classes in terms of their magnitudes $\left|\frac{\partial \mathrm{I}}{\partial \mathrm{l}_i}(p)\right|$. If two clusters have the same size, the image point p is balanced.

The sorting method proposed in [4] to classify $\left\{\frac{\partial \mathrm{I}}{\partial \mathrm{l}_i}(p)\right\}_{i=1}^{N}$ can be generalized to extract 3D imbalanced vertices with normal vector projections. Let $\mathrm{maxDiff}$ be the max difference and D be the index of maximum difference:

$$\mathrm{maxDiff} = \max_j(\beta_{j+1} - \beta_j)$$

$$\mathrm{D} = \operatorname{argmax}_j(\beta_{j+1} - \beta_j)$$

Where β represents projected vectors, and $1 \leq \mathrm{j} \leq \mathrm{N} - 1$. Given a threshold on homogeneity ε, the imbalanced vertex can be defined under the condition that $\mathrm{maxDiff} < \varepsilon$:

$$\mathrm{IMB}(\mathrm{v}_i) = \begin{cases} 1 & D_i < \frac{N}{2} \\ 0 & else \end{cases}$$

4.2. Keypoints based Feature Sensitive Mesh Subdivision

Based on imbalanced keypoints detection, all the vertices are classified into two categories. According to the properties of imbalanced vertices, our keypoints distributed mainly at the boundaries and detailed parts, which should be remained after subdivision but slightly adjusted with neighbors. We propose a subdivision scheme, which contains edge point generation and smooth operator, to balance the emphasis of original features and smoothing extent.

The unit of edge point generation in our provided method is a couple of triangles back to back as illustrated in Figure 8. Denote the edge point generator in Feature Sensitive Subdivision and Advanced Feature Sensitive Subdivision as $G_{FSS}(N)$ and $G_{AFSS}(N)$ respectively, where N is the set of neighbor points.

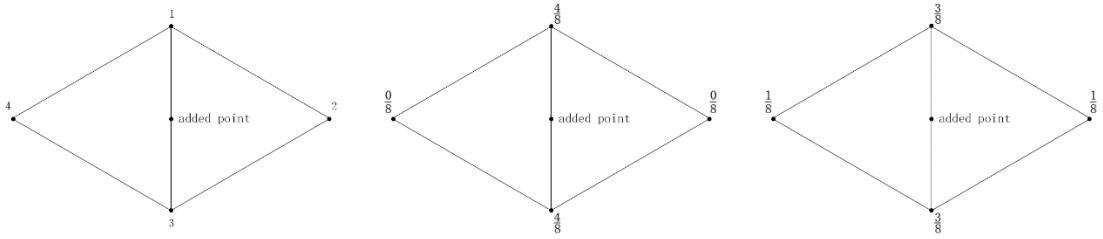

Figure 8 Unit of edge point generation (left) Feature Sensitive Subdivision edge point generator (middle). Advanced Feature Sensitive Subdivision edge point generator (right)

The balance can be guided by the amount of imbalanced keypoints in an isolated generation unit and implemented by a weighted combination of $G_{FSS}(N)$ and $G_{AFSS}(N)$. For a precise and accurate calculation, the weight of two generators should be geometrically related and geometrically symmetric. The weight of $G_{FSS}(N)$ and $G_{AFSS}(N)$ will be defined as $\mathrm{W}_{G_{FSS}}$ and $\mathrm{W}_{G_{AFSS}}$, which depend on the number of keypoints in a generation unit, and obey the following principles.

$$\mathrm{W}_{G_{FSS}} = \sum_{i=1}^{|N|} Key(N_i)$$

$$\mathrm{W}_{G_{AFSS}} = |N| - \sum_{i=1}^{|N|} Key(N_i)$$

$$\mathrm{Key}(N_i) = \begin{cases} 1 & N_i \ is \ a \ keypoint \\ 0 & N_i \ isn't \ a \ keypoint \end{cases}$$

A combination of two edge point generator $G(N)$ will be defined

$$G(N) = \mathrm{W}_{G_{FSS}} G_{FSS}(N) + \mathrm{W}_{G_{AFSS}} G_{AFSS}(N)$$

Smooth operator will also be guided by keypoints, which extends the previous smooth operator. Neighbor vertices for smooth operator will be different which depends on whether the centroid vertex is a keypoint or not. If so, neighbor vertices should be elder one-ring vertices on M_i, else, one-ring vertices on M_{i+1}.

5. Experiment

We test different subdivision methods on several biomedical data, including phalanx (distal phalanx, middle phalanx, and proximal phalanx), cuneiform bone (intermediate cuneiform bones, entocuneiform, ectocuneiform), central anlrle bone, cuboid bone and so on provided by Florida State University.

As the time of subdivision methods iteration increased, the performance of different algorithm is becoming easier to differentiate, as illustrated in Figure 9. Except Catmull method, all the subdivision methods implement one to four triangular faces subdivision, which means each mesh in a row has the same number of vertices and faces, except Catmull subdivision. The number of vertices and triangular faces in each iteration follows the principle when apply one to four mesh subdivision schemes.

$$V(M_i) = V(M_{i-1}) + \frac{3}{2} F(M_{i-1})$$

$$F(M_i) = 4V(M_{i-1})$$

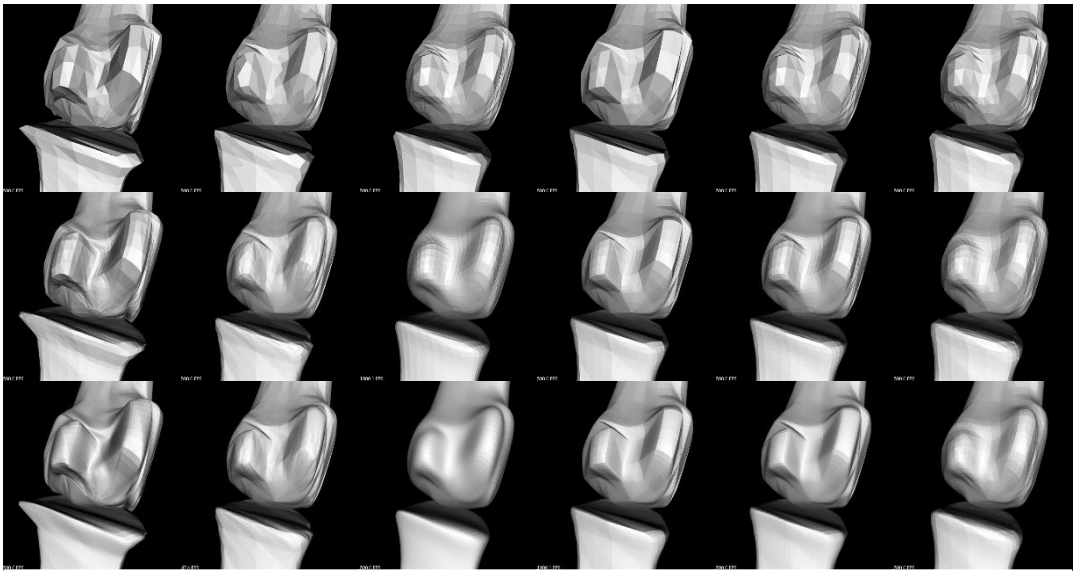

a1	b1	c1	d1	e1	f1
a2	b2	c2	d2	e2	f2
a3	b3	c3	d3	e3	f3

Figure 9 Subdivision Comparison on same biomedical data. a) Butterfly Subdivision. b) Catmull Subdivision. c) Loop Subdivision. d) Edge Sensitive Subdivision. e) Advanced Edge Sensitive Subdivision. f) Keypoints-based Edge Sensitive Subdivision. Iteration time increase by row.

Obviously, subdivision result after Loop method has a better spherical resembling appearance, while Feature Sensitive Subdivision provide a better property of edge feature remaining. Butterfly subdivision leads mesh to a more boundary malleable shape, while Catmull present more vertex details. Advanced Feature Sensitive Subdivision accomplish an edge feature remaining and smooth result, but compared with Keypoint-based Feature Sensitive Subdivision, the later algorithm provides a better result.

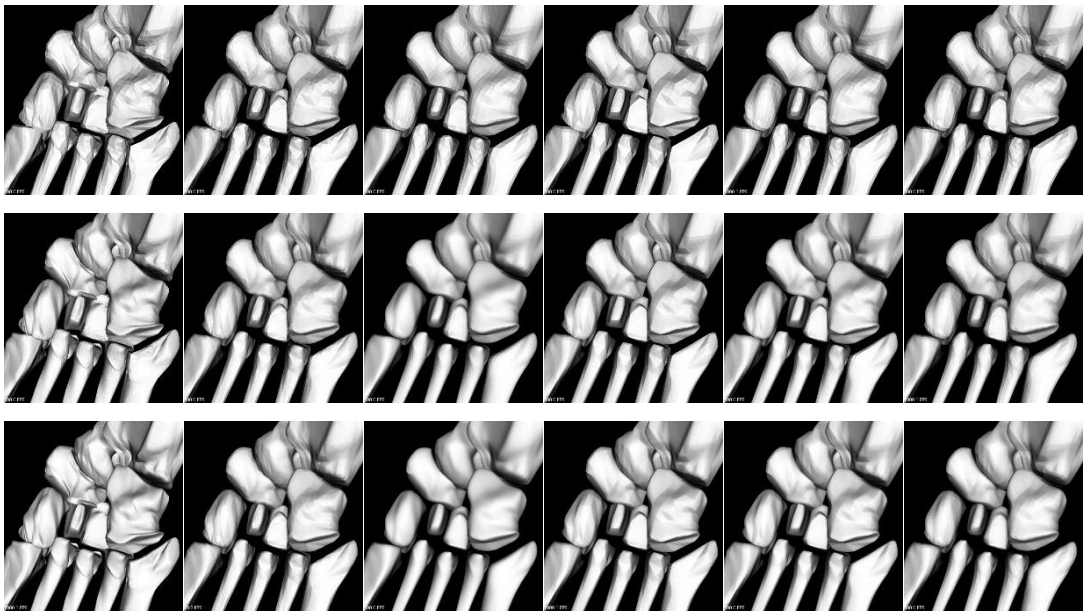

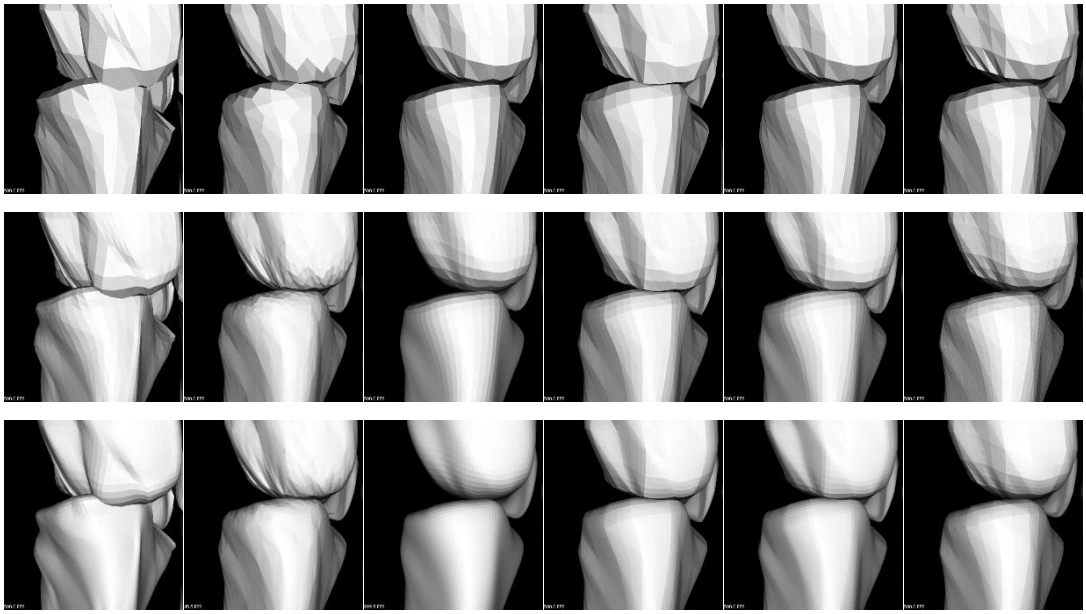

6. Conclusion

Proposed Feature Sensitive Subdivision method works well on edge features but it will generate troublesome model-shape noise waves. By using the idea in Advanced Feature Sensitive Subdivision, noise waves problem will be solved and generate a smoother result. Compared all the methods mentioned in the figures, keypoints-based Feature Sensitive Subdivision has a better feature based result.

7. Reference

[1] CT. Loop. Smooth subdivision surfaces based on triangles. Masters thesis. University of Utah, Dept. of Mathematics. 1987.

[2] E. Catmull, and J Clark. Recursively generated B-spline surfaces on arbitrary topological meshes. Computer-Aided Design. 1978.

[3] Butterfly

[4] Q. Li, J. Ye, and C. Kambhamettu. Interest point detection using imbalance oriented selection. Pattern Recognition,

[5] K. Feng, Q. Li, Y. Gong, J. Yang. Detection of imbalanced vertices in 3D meshes.

[6] Tao Ju. Subdivision meshes for organizing spatial biomedical data.

[7] A. Amresh, G. Farin. A. Razdan, “adaptive subdivision Schemes for triangle Meshes”, Arizona State University, October 5, 2000.

[8] D. Rose, M. Kada, T. Ertl,“On-the-Fly Adaptive Subdivision Terrain”, VMV 2001, pp.87-92, 2001.

[9] L. Kobbelt. “ 3 Subdivision”, SIGGRAPH ’00 Proceedings, pp. 103-112, 2000.

[10] S. Seeger, K. Hormann, G. Hausler, G. Greiner, “A Sub-Atomic Subdivision Approach”, VMV 2001,Stuttgart, Germany, 77-86, 2001.
[11] Z. Xu, K. Kondo, “Adaptive refinements in subdivision surfaces”, Eurographics'99, Short papers and demos, 239-242, 1999.
[12] X. Tao. Application of 3D Reconstruction in Maxillofacial Surgery. Acta Universitatis Medictnae Tangi. 1999.
[13] JF. Deng. FPGA accelerate 3D CT reconstruction. Application of Electronic Technique. 2010.
[14] PD. Groeve. Registration of 3D Photographs with Spiral CT images for Soft Tissue Simulation in Maxillofacial Surgery. Medical Image Computing & Computer-assisted int.. 2001.
[15] C Sun. Parallel 3D-CT Reconstruction Using MPI. Computer Engineering & Applications. 2006.
[16] J. Carson, T. Ju, H. Lu, C. Thaller, M. Xu, S. Pallas, M. C. Crair, J. Warren, W. Chiu and G. Eichele. A Digital Atlas to Characterize the Mouse Brain Transcriptome. PLoS Computational Biology, to appear, 2005.
[17] Carson, J. P., Thaller, C., and Eichele, G. (2002) A transcriptome atlas of the mouse brain at cellular resolution. Curr. Opin. Neurobiol. 12, 562–565.
[18] Lein, E., Hawrylycz, M., et al.: Genome-wide atlas of gene expression in the adult mouse brain. Nature 445(7124), 168–176 (2007)
[19] Christiansen, J.H., Yang, Y., Venkataraman, S., Richardson, L., Stevenson, P., Burton, N., Baldock, R.A., Davidson, D.R.: Emage: a spatial database of gene expression patterns during mouse embryo development. Nucleic Acids Research 34, 637–641 (2006)
[20] T. Ju, J. Warren, G. Eichele, C. Thaller, W. Chiu, J. Carson, A geometric database for gene expression data, in: Proc. Eurographics/ACM SIGGRAPH Symposium on Geometry Processing, Eurographics Association, 2003, pp. 166–176.
[21] S. Schaefer, J. Hakenberg, J. Warren, Smooth subdivision of tetrahedral meshes, in: Proc. the Eurographics/ACM SIGGRAPH Symposium on Geometry Processing, Eurographics Association, 2004, pp. 151–158.
[22] T.W. Sederberg, S.R. Parry, SIGGRAPH Comput. Graph. 20 (4) (1986) 151–160.
[23] Bonev B, Cavalli G. Organization and function of the 3D genome[J]. Nature Reviews Genetics, 2016, 17(11): 661-678.
[24] Tjong H, Li W, Kalhor R, et al. Population-based 3D genome structure analysis reveals driving forces in spatial genome organization[J]. Proceedings of the National Academy of Sciences, 2016, 113(12): E1663-E1672.
[25] Caspermeyer J. Principles of 3D Genome Folding and Gene Expression Studied across Species[J]. Molecular Biology and Evolution, 2017, 34(6): 1548-1548.
[26] Koopman D, Dalen J, Arkies H, et al. A small voxel FDG-PET/CT reconstruction improves the visual evaluation of axillary lymph nodes in patients with breast cancer[J]. Journal of Nuclear Medicine, 2016, 57(supplement 2): 1502-1502.
[27] Muthusami P, Shkumat N, Rea V, et al. CT reconstruction and MRI fusion of 3D rotational angiography in the evaluation of pediatric cerebrovascular lesions[J]. Neuroradiology, 2017: 1-9.
[28] McCann M T, Nilchian M, Stampanoni M, et al. Fast 3D reconstruction method for

differential phase contrast X-ray CT[J]. Optics express, 2016, 24(13): 14564-14581.
[29] Bærentzen J A, Abdrashitov R, Singh K. Interactive shape modeling using a skeleton-mesh co-representation[J]. ACM Transactions on Graphics (TOG), 2014, 33(4): 132.
[30] Guskov I V, Schröder P, Sweldens W. Non-uniform relaxation procedure for multiresolution mesh processing: U.S. Patent 8,830,235[P]. 2014-9-9.
[31] Zhang Y, Ma L. A Scaling Method of Sensitive Objects Based on Loss Constraint Triangle Mesh Deformation[J]. Journal of Image and Graphics, 2015, 3(2).
[32] Xie Q, Sze K Y, Zhou Y X. Drape simulation using solid-shell elements and adaptive mesh subdivision[J]. Finite Elements in Analysis and Design, 2015, 106: 85-102.
~~[22]~~[33] Liu H H. An Improved refinement algorithm of triangular mesh subdivision based on minimum weight theory[C]//Applied Mechanics and Materials. Trans Tech Publications, 2014, 513: 2552-2555.